PCP
PLANT & CELL PHYSIOLOGY

# miR396a-Mediated Basic Helix–Loop–Helix Transcription Factor *bHLH74* Repression Acts as a Regulator for Root Growth in Arabidopsis Seedlings

Maolin Bao[1,3], Hongwu Bian[1,3], Yulong Zha[1], Fengyun Li[1], Yuzhe Sun[1], Bin Bai[1], Zhehao Chen[1,2], Junhui Wang[1], Muyuan Zhu[1] and Ning Han[1,*]

[1]Key Laboratory for Cell and Gene Engineering of Zhejiang Province, Institute of Genetics, College of Life Sciences, Zhejiang University, Hangzhou 310058, Zhejiang, China
[2]College of Life and Environmental Sciences, Hangzhou Normal University, Hangzhou, 310036, Zhejiang, China
[3]These authors contributed equally to this work.
*Corresponding author: E-mail, ninghan@zju.edu.cn; Fax, +86-571-88206535.
(Received September 17, 2013; Accepted April 15, 2014)

**miR396 targets seven *GROWTH-REGULATING FACTOR* (*GRF*) genes and the *BASIC HELIX–LOOP–HELIX* (*bHLH*) *TRANSCRIPTION FACTOR 74* gene (*bHLH74*) in Arabidopsis. Previous research revealed that the miR396 target module regulates cell proliferation and plays a critical role in leaf development. However, no additional biological functions of miR396 have been investigated in detail. In this study, T-DNA insertion mutants and transgenic plants with altered levels of miR396 or its target genes were used to characterize the regulatory role of miR396 in root development. We found that *AtMIR396a* was the predominant source for miR396 accumulation in the roots of seedlings, and that the *mir396a-1* mutant had longer roots than wild-type seedlings. Overexpression of *AtMIR396a* decreased the transcript levels of target genes such as *GRF* genes and *bHLH74*, and resulted in a shorter root phenotype. Furthermore, the *bhlh74-1* mutant had shorter roots, whereas overexpression of an miR396-resistant form of *bHLH74* (*mbHLH74*) had an enhanced root growth phenotype. Moreover, *MIR396a* regulated root growth by affecting the elongation zone. Taken together, these data indicate that miR396a-mediated *bHLH74* repression helps regulate root growth in Arabidopsis seedlings.**

**Keywords:** *Arabidopsis thaliana* • Basic helix–loop–helix (bHLH) transcription factor 74 (bHLH74) • Growth-regulating factor (GRF) • miRNA396 • Root growth.

**Abbreviations:** bHLH, basic helix–loop–helix; CaMV, *Cauliflower mosiac virus*; GRF, growth-regulating factor; GUS, β-glucuronidase; miRNA, microRNA; qRT-PCR, quantitative real-time PCR; RISC, RNA-induced silencing complex; STTM, short tandem target mimic.

## Introduction

microRNAs (miRNAs), which are approximately ~21 nucleotides (nt) in size, are key players in the gene regulatory networks of eukaryotes. In plants, miRNAs are processed from stem–loop regions of long primary transcripts by a Dicer-like enzyme, and loaded into RNA-induced silencing complexes (RISCs), where they generally direct cleavage of complementary mRNAs or play a role in translation inhibition (Jones-Rhoades et al. 2006). miRNAs have been demonstrated to play crucial roles in various biological processes including plant development, hormone signaling and stress responses (Rubio-Somoza et al. 2009, Voinnet 2009).

The Arabidopsis root is an attractive system for the study of plant organogenesis because of the simplicity of its organization. Recent studies have revealed that in addition to transcription factors and plant hormones, small non-coding RNAs play critical roles in root development. For example, miR164-mediated *NAC1* (NAM/ATAF/CUC *domain transcription factor 1*) repression down-regulates auxin signals for lateral root emergence in Arabidopsis (Guo et al. 2005). In addition to miR160 acting as a key controller of root cap cell formation through repression of the *AUXIN RESPONSE FACTOR* (*ARF*) genes *ARF10* and *ARF16* (Wang et al. 2005), it also targets *ARF17* to regulate adventitious root initiation (Gutierrez et al. 2009). miR390, TAS3-derived *trans*-acting short-interfering RNAs (tasiRNAs) and ARFs form an auxin-responsive regulatory network controlling lateral root growth (Marin et al. 2010, Yoon et al. 2010). It was also reported that interaction of miR393 with *TIR1* (*transport inhibitor response protein 1*) modulates auxin sensitivity and affects primary root growth and lateral root emergence (Chen et al. 2011). Furthermore, miR393 can

*Plant Cell Physiol.* 55(7): 1343–1353 (2014) doi:10.1093/pcp/pcu058, available online at www.pcp.oxfordjournals.org

target *AFB3* (*AUXIN SIGNALING F-BOX 3*) to control root system architecture in response to external and internal nitrate availability in Arabidopsis (Vidal et al. 2010). Recently, a novel regulatory pathway involving bidirectional cell signaling mediated by miR165/miR166 and the transcription factors SHR (SHORT ROOT)/SCR (SCARECROW) has been identified as determining root cell fate (Carlsbecker et al. 2010). Therefore, development of the Arabidopsis root is a dynamic process, which requires the integration of plant hormones, transcriptional regulators and small RNAs to produce the correct developmental outcome (Meng et al. 2010).

miRNA396 has been implicated as a significant regulator of cell proliferation (Rodriguez et al. 2010). In Arabidopsis, the miRNA396 family consists of two members: miR396a and miR396b, which are encoded by *AtMIR396a* and *AtMIR396b*, respectively. Mature miR396a and miR396b differ in sequence by one nucleotide at the 3′ end, with a G in miR396a and a U in miR396b. Seven conserved targets belonging to the *GROWTH-REGULATING FACTOR* (*GRF*) family of transcription factors have been validated as targets of miRNA396 (Jones-Rhoades and Bartel 2004, Jones-Rhoades et al. 2006). GRF proteins are transcriptional regulators involved in leaf and cotyledon development (Kim et al. 2003, Horiguchi et al. 2005, Kim and Lee 2006, Lee et al. 2009). Mutations in different *GRF* genes, or overexpression of miR396, produce narrow-leaf phenotypes through a reduction in cell number (Liu et al. 2009, Rodriguez et al. 2010). miR396 can regulate cell proliferation and the size of the meristem through regulation of *GRF* genes, and the balance between miR396 and *GRF* genes controls the final number of cells in leaves (Rodriguez et al. 2010). Target prediction, combined with RACE (rapid amplification of cDNA ends)-PCR mapping of target mRNA cleavage sites, led to identification of another target, *bHLH74* (Debernardi et al. 2012). *bHLH74* encodes a basic helix–loop–helix (bHLH) transcription factor. Repression of *bHLH74* by miR396 is required for margin and vein pattern formation in Arabidopsis leaves (Debernardi et al. 2012). More recently, functional characterization of miR396 in the legume *Medicago truncatula* revealed that miR396 affects mycorrhization and root meristem activity (Bazin et al. 2013). However, in Arabidopsis, the biological role of miR396 in root development remains unclear.

In this study, we report that *MIR396a* participates in the regulation of root growth, *AtMIR396a* is the predominant source of miR396 accumulation in seedling roots and miR396a-mediated *bHLH74* repression negatively regulates the root cell elongation zone.

## Results

### mir396a-1 mutants exhibit longer roots than wild-type plants

To discover the biological function of miR396 in root development, a T-DNA insertion mutant of *AtMIR396a* was obtained from the Arabidopsis Biological Resource Center. PCR-assisted genotyping revealed that the T-DNA in *mir396a-1* (SALK_064067) was inserted 449 bp upstream of the *AtMIR396a* precursor (**Fig. 1A**). Quantitative real-time PCR (qRT-PCR) revealed that the level of *AtMIR396a* primary transcript was 50% lower in homozygous seedlings of the mutant than in the wild type (**Fig. 1A**), indicating that it is a knockdown mutant of *AtMIR396a*. The level of mature miR396 in the *mir396a-1* mutant was determined; the miR396 accumulation in the roots was 20% that of the wild type. In leaf tissues, the level of miR396 in *mir396a-1* decreased to 58% of that of the wild type (**Fig. 1B**). These data indicate that miR396 arises primarily from *AtMIR396a* in Arabidopsis roots. Next, root growth was observed in *mir396a-1*. The primary root length of 5-day-old *mir396a-1* seedlings was significantly longer than that of the wild type (**Fig. 1C, D**). To test whether the root phenotype of *mir396a-1* was caused by a decreased miR396a level, a complementation experiment was carried out by generating *pMIR396a:MIR396a* (in the *mir396a-1* background) transgenic lines. We found that these transgenic lines displayed normal root growth as in controls (**Fig. 1B, C**), confirming that this construct is sufficient to complement the *mir396a-1* mutant phenotype. To confirm the effect of reduced miR396 function, we also used a short tandem target mimic (STTM) strategy to generate *35S:STTM396* transgenic lines with inhibited miR396 activity (Tang et al. 2012, Yan et al. 2012). The *35S:STTM396* seedlings displayed longer root growth than observed for seedlings containing the empty vector control ($P < 0.01$) (**Fig. 2A, B**). Compared with the wild type, the level of mature miR396 was decreased, while transcript levels of miR396 targets including *GRF1*, *GRF2*, *GRF3* and *bHLH74* were increased in *35S: STTM396* transgenic lines (**Fig. 2C, D**). These results imply that *AtMIR396a* might be involved in the regulation of primary root growth.

### 35S:MIR396a transgenic lines exhibit short-root phenotypes

To investigate the biological function of miR396 and its targets, transgenic lines overexpressing *AtMIR396a* under the control of the constitutive *35S* promoter were generated. Twenty-one independent homozygous *35S:MIR396a* $T_3$ lines were obtained. Small RNA blot analysis revealed elevated miR396 levels in the transgenic lines *35S:MIR396a #7*, *#17* and *#21*, but not in the line *#24* (**Fig. 2A**).

Overexpression of *MIR396a* resulted in a short-root phenotype (**Fig. 2B, C**). Primary root elongation of *35S:MIR396a* seedlings was much reduced. The roots of wild-type seedlings were 16.20 ± 3.87 mm (mean ± SD, $n = 20$) after 5 d growth on B5 medium, whereas roots of the *35S:MIR396a* lines *#7*, *#17* and *#21* were 6.20 ± 1.06, 7.10 ± 1.28 and 6.90 ± 0.12 mm (mean ± SD, $n = 20$), respectively. There was no significant difference in primary root length between *35S:MIR396a #24* and the wild type (**Fig. 2D**). In combination with Northern blot results (**Fig. 2A**), this indicates that the short-root phenotype correlated with increased levels of miR396 in these transgenic lines. In addition to shorter roots, *35S:MIR396a* plants developed more

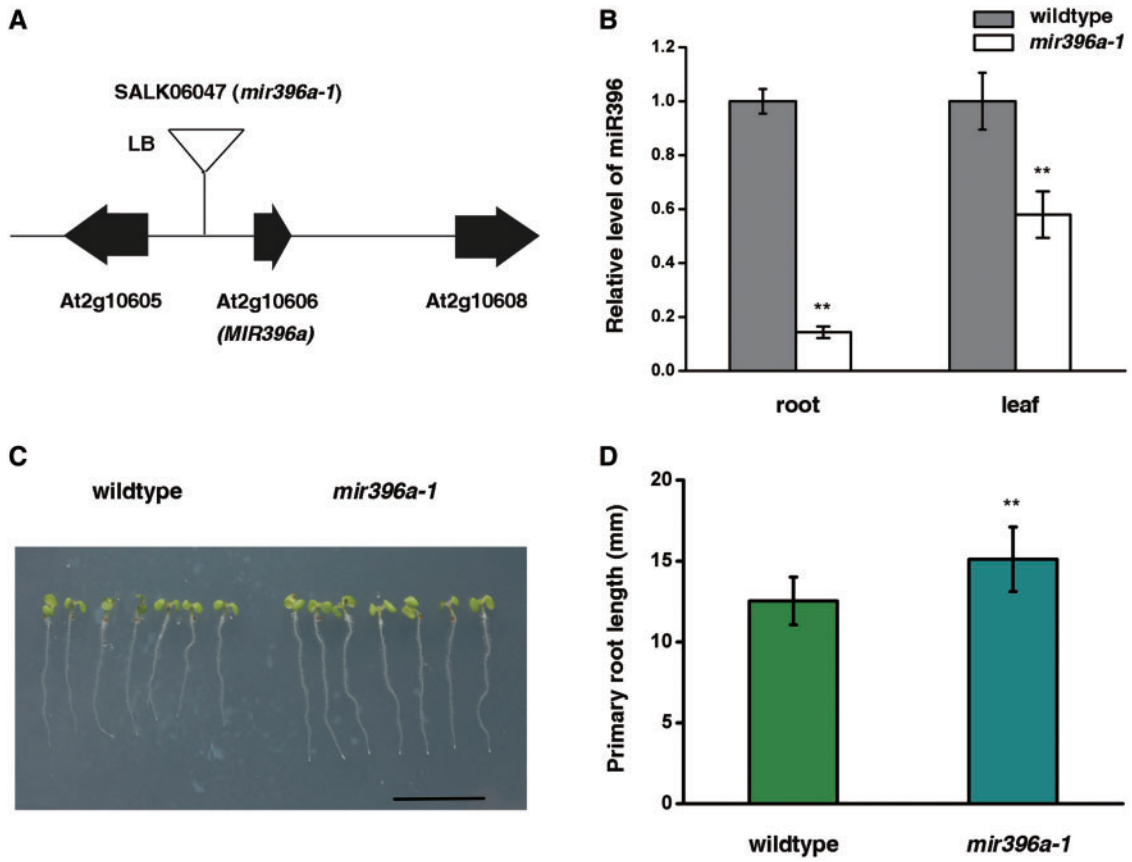


**Fig. 1** Characterization of a T-DNA insertion mutant of *AtMIR396a*. (A) The *AtMIR396a* locus showing the T-DNA insertion corresponding to the SALK_064067 line. The insertion site (open triangle) for the left border (LB) of *mir396a-1* is shown. The arrows indicate the *AtMIR396a* precursor and the genes flanking *AtMIR396a* as annotated in GenBank. The schematic is not drawn to scale. (B) miR396a levels in 10-day-old wild-type and *mir396a-1* seedlings. Quantifications were normalized to the level of miR171a, which is relatively abundant and constant across the tested tissues. The expression levels in wild-type plants were set to 1.0. Error bars represent the SD. Double asterisks indicate a significant (ANOVA, $P < 0.01$) difference from the wild type. (C) Root morphology of 5-day-old wild-type and *mir396a-1* seedlings. Scale bar = 1 cm. (D) Primary root length of 5-day-old wild-type and *mir396a-1* seedlings. Error bars represent the SD. Double asterisks indicate a significant (ANOVA, $P < 0.01$) difference from the wild type.

elongated root hairs relative to the wild type (**Fig. 2C**). Overexpression of miR396a resulted in a leaf phenotype similar to that described in previous studies (Liu et al. 2009, Rodriguez et al. 2010), with the area of the fourth leaf in *35S:MIR396a* lines decreased compared with the wild type (**Fig. 3**).

qRT-PCR methodology was used to analyze RNA levels of the target genes *GRF1*, *GRF2*, *GRF3*, *GRF4*, *GRF9* and *bHLH74* in the transgenic plants. Primers used were designed from each side of the miR396 cleavage site to detect uncleaved mRNA. qRT-PCR analysis revealed that transcript levels of the *GRF* genes and *bHLH74* in root tissues were greatly down-regulated in *35S:MIR396a* lines *#7* and *#17* compared with the wild type (**Fig. 2E**).

## MIR396 family and its four targets have transcriptional activities in root tissues

To view the expression regions of *MIR396a* and *MIR396b*, promoter–reporter constructs were generated by fusing 2 kb upstream regulatory sequences to a β-glucuronidase (GUS) reporter gene. In roots, GUS staining was observed in the vascular bundle of the primary root from the hypocotyl to the elongation zone, and extended slightly into the meristematic zone (**Fig. 3A, B**). GUS expression was also observed in the emerging lateral roots of *proMIR396a:GUS* plants (**Fig. 3C**). In leaves, both *MIR396a* and *MIR396b* reporters were expressed in the whole leaf area, and presented a proximodistal gradient in young leaves, with higher levels in the distal than the proximal parts (**Fig. 4A, B**). The spatial transcriptional patterns of *MIR396a* and *MIR396b* were similar to each other in seedlings.

Promoter reporter lines were also used to observe expression patterns of *bHLH74* and *GRF* genes during root development. These genes displayed different transcriptional patterns in root tissues. GUS staining revealed that the *bHLH74* promoter was strongly active in the vascular bundle of primary and emerging lateral roots (**Fig. 3D, E**), indicating overlapping

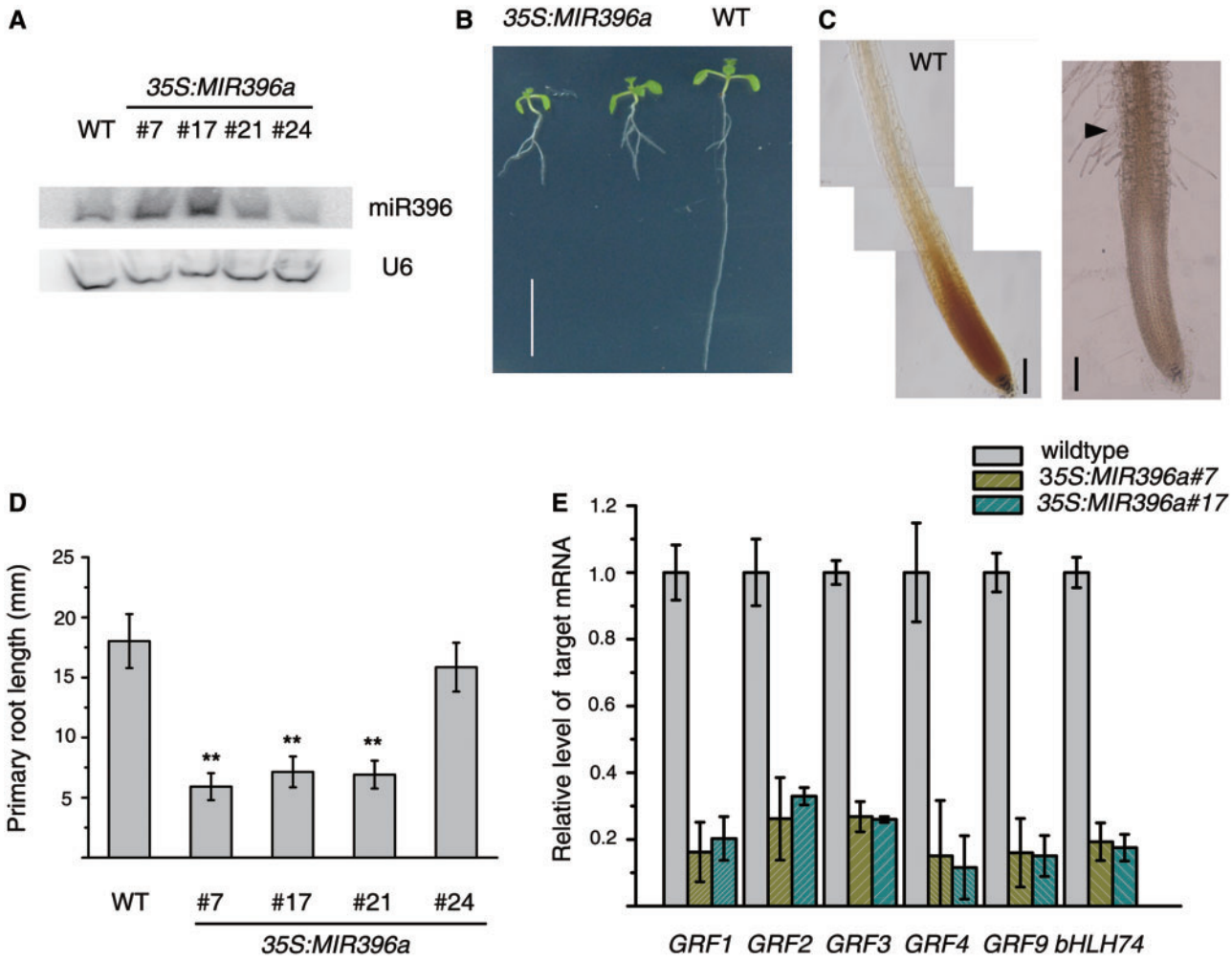


**Fig. 2** *35S:MIR396a* transgenic lines present a short-root phenotype. (A) Overexpression of miR396 in transgenic Arabidopsis plants. RNA gel blot analysis of miR396 levels in the wild type and four representative *35S:MIR396a* transgenic lines. A 30 μg aliquot of total RNA was loaded and U6 small nuclear RNA (snRNA) was used as a loading control. (B) Root morphology of 5-day-old wild-type and *35S:MIR396a* seedlings grown on B5 agar plates. Scale bar = 1 cm. (C) Lugol-stained roots of the wild type (left) and *35S:MIR396a #7* (right) at 5 d after germination. Scale bar = 1 cm. The arrowhead indicates the root hairs of *35S:MIR396a #7*. (D) Primary root length of 5-day-old wild-type and *35S:MIR396a* seedlings. Error bars represent the SD. Double asterisks indicate a significant (ANOVA, $P < 0.01$) difference from the wild type. (E) Relative transcript levels of *GRF* genes and *bHLH74* in *35S:MIR396a* transgenic lines. RNA was isolated from roots of 5-day-old seedlings. The data shown are means ± SD of three biological replicates. Quantifications were normalized to the expression of AT4G33380, which was validated as the most stable gene for our experiments (Czechowski et al. 2005). Expression levels are shown relative to those of wild-type plants (set to 1.0).

expression regions with *MIR396*. *proGRF2:GUS* expression was localized to the root tips (**Fig. 3F**), whereas the GUS signal in *proGRF4:GUS* seedlings was strong in the meristematic zone, but weak in the elongation zone (**Fig. 3G**). *proGRF9:GUS* expression was detected in the elongation and differential zone, and gradually disappeared in the meristematic zone (**Fig. 3H**). In contrast, RT-PCR data indicated that expression of *GRF8* and *GRF7* was very weak in the root (**Fig. 5**); this is consistent with previous RNA gel blot data (Kim et al. 2003). The above observations, combined with a previous report on *GRF1* and *GRF3* (Kim et al. 2003), show that at least six (*bHLH74* and *GRF1*, *2*, *3*, *4* and *9*) of the miR396 targets have transcriptional activities in root tissues.

## bHLH74 is involved in miR396-directed root growth regulation

Previous research has shown that *grf1*, *grf2*, *grf3*, *grf4* and *grf5* mutants have normal roots (Kim et al. 2003, Debernardi et al. 2012). In this study, we measured the root lengths of *grf1grf2grf3* and *grf4* mutants. Additionally, the T-DNA insertion line *grf9-1* (SALK_140746C), with no detectable expression of *GRF9* (**Figs. 6**), also had its root phenotype observed. The primary root growth in *grf1grf2grf3*, *grf4* and *grf9-1* appeared normal compared with the wild type (**Table 1**). Taken in conjunction with the evidence that expression levels of *AtGRF7* and *AtGRF8* in roots of wild-type seedlings were low, this raised the

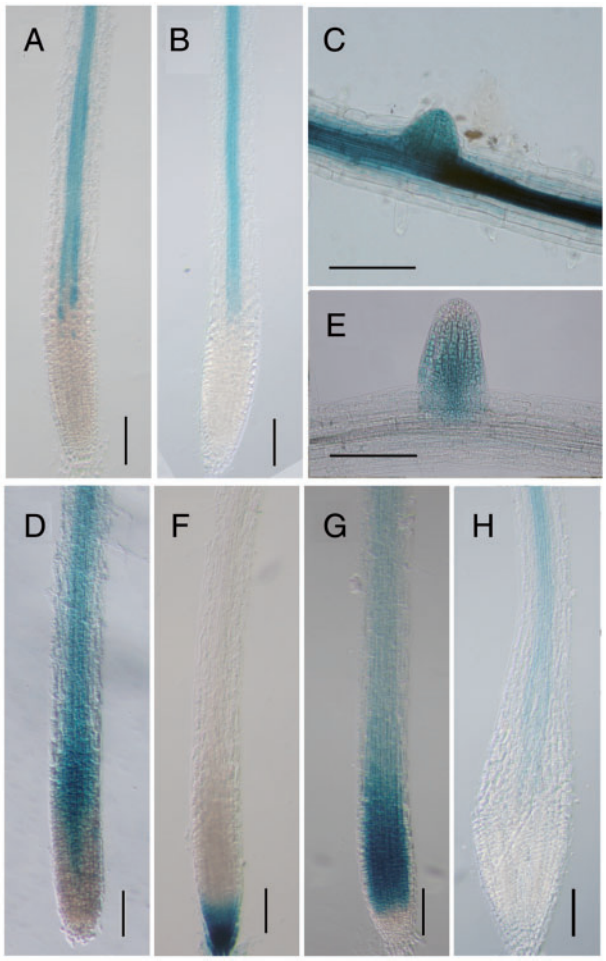


**Fig. 3** GUS staining patterns in the roots of 10-day-old Arabidopsis transformants carrying *promoter:GUS* reporter gene constructs. (A and C) *proMIR396a:GUS* plants: (A) primary root; (C) lateral root. (B) *proMIR396b:GUS*. (D and E) *probHLH74:GUS*: (D) primary root; (E) lateral root. (F) *proGRF2:GUS*. (G) *proGRF4:GUS*. (H) *proGRF9:GUS*. Scale bars = 1 mm.

possibility that *bHLH74* may be involved in regulating root growth of seedlings.

To define the function of bHLH74 in root growth regulation, the T-DNA insertion mutant *bhlh74-1* (GABI-Kat 720G11) was used to observe the root phenotype. Meanwhile, a modified version of *bHLH74* (*mbHLH74*) with mutations that impaired its interaction with miR396 was designed and used to generate *35S:mbHLH74* transgenic plants (**Fig. 4A**). RT-PCR revealed that *bHLH74* transcript levels increased in *35S:mbHLH74 #8* and *#11*. In contrast, no *bHLH74* transcript was detected in the root of the *bhlh74-1* mutant (**Fig. 4B**). Compared with the wild type, the primary root length increased by 18.16% in *35S:mbHLH74* (**Fig. 4C**), while it decreased by about 24.07% in *bhlh74-1* 5 d after germination (**Fig. 4D**). These results support the hypothesis that *bHLH74* is an miR396 target of major importance involved in root growth regulation.

## MIR396a regulates root length by affecting the elongation zone

To investigate how *MIR396a* regulates root development, root meristems were observed using propidium iodide-stained roots from wild-type, *mir396a-1*, *35S:MIR396a*, *bhlh74-1* and *35S:mbHLH74* seedlings (**Fig. 5A–E**). Only slight changes in meristem cell number and meristem length were detected in the mutant plants (**Fig. 5F, G**). Next, the impact of miR396-mediated regulation on cell proliferation was analyzed. The levels of *CYCLINB1; 1* (*CYCB1; 1*) and *KNOLLE*, which are known to be expressed during mitosis (Lukowitz et al. 1996, Menges et al. 2005), were detected by qRT-PCR. This revealed that the expression of these cell cycle-related genes was not significantly affected by miR396a levels (**Supplementary Fig. S7**).

The elongation zone was observed in these lines. This revealed that the length of the elongation zone was significantly increased in *mir396a-1* and *35S:mbHLH74*, but was decreased in *35S:MIR396a* transgenic plants (**Fig. 6A–C**). The length of differentiated root cells was measured in the wild type, *mir396a-1*, *35S:MIR396a*, *bhlh74-1* and *35S:mbHLH74* to analyze how miR396a controls cellular elongation. We found that mature cortical cell length was increased in *mir396a-1*, but was decreased in *35S:MIR396a* and *bhlh74-1* (**Fig. 6D**). These data indicate that miR396 can regulate root growth by affecting the elongation zone.

## Discussion

An miR396 target module is known to play a critical role in leaf development. It was recently reported that the miR396–*GRF1/GRF3* regulatory module acts as a developmental regulator in the reprogramming of root cells during cyst nematode infection (Hewezi et al. 2012). The results of this study demonstrate that *MIR396a* has an additional function as a regulator of root growth in Arabidopsis seedlings, through an interaction with *bHLH74*.

Use of promoter:GUS reporter lines revealed that *AtMIR396a* and *AtMIR396b* had similar spatial transcriptional patterns in roots, although their expression is driven by different promoters (**Fig. 3**). Analysis of the *mir396a-1* mutant revealed that miR396a contributes more than miR396b to root development, with the level of mature miR396 in the root greatly decreased in the *mir396a-1* mutant (**Fig. 1**). Northern blot analysis and sequencing data provided by Jeong et al. confirmed that the two miR396 family members had different expression patterns; while miR396a was preferentially expressed in the root, miR396b was preferentially expressed in the flower (Jeong et al. 2013). The effect of the mutation in *AtMIR396a* seems not to be restricted to within the vascular bundle tissue. This indicates that the GUS reporter assay can only reflect the transcriptional regions of *MIR396*, which might be different from the spatial accumulation of mature miR396. Small RNA deep-sequencing profiles using green fluorescent protein (GFP) marker lines provided detailed expression patterns of

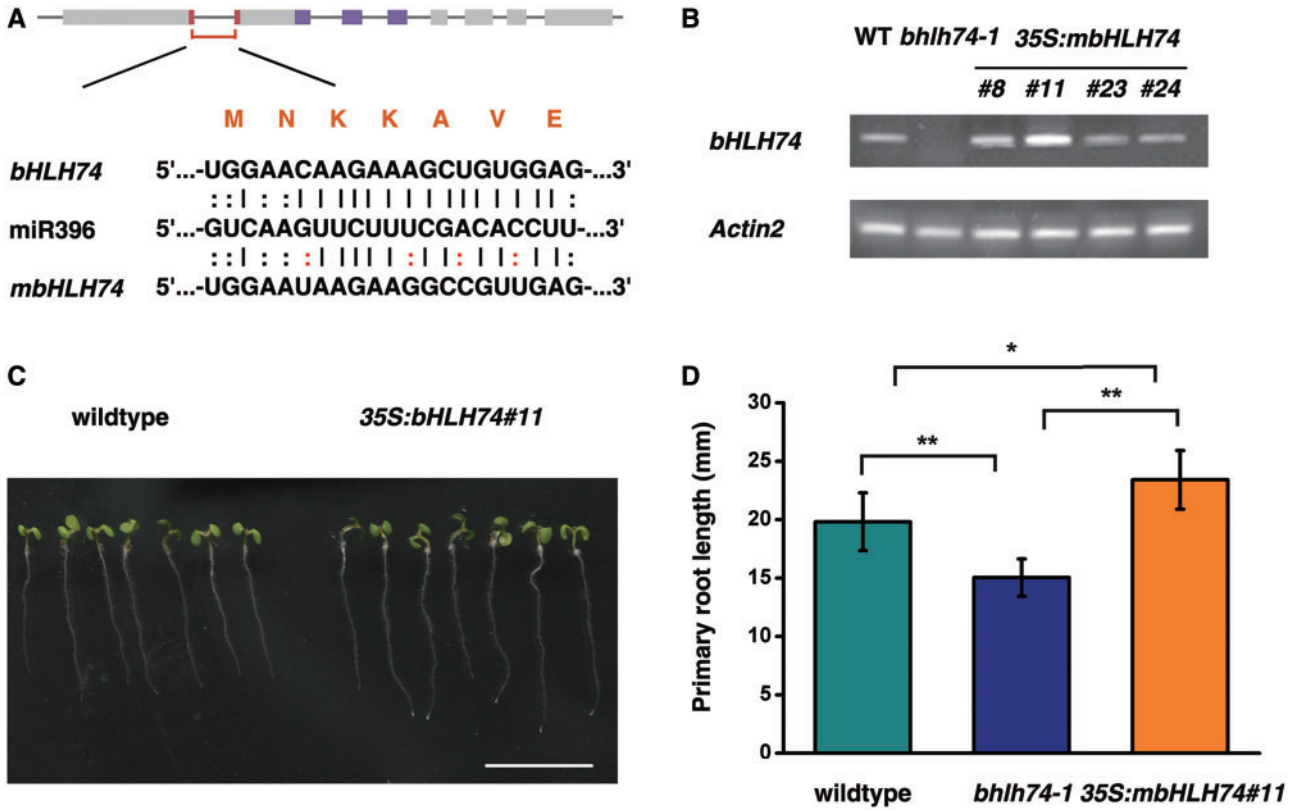


**Fig. 4** miR396-mediated *bHLH74* regulation affects root growth. (A) Diagram of *mbHLH74* expression constructs. The introduced point mutations in the miR396 target site of *bHLH74* are shown. (B) Semi-quantitative RT-PCR analysis of *bHLH74* transcript levels in wild-type, *bhlh74-1* and *35S:mbHLH74* (*#8*, *#11*, *#23* and *#24*) plants. The *ACTIN2* gene was used as an internal control. (C) Root phenotype of 5-day-old wild-type and *35S:mbHLH74* transgenic plants. Scale bar = 1 cm. (D) Primary root length of 5-day-old wild-type and *35S:mbHLH74* plants. Error bars represent the SD. Asterisks indicate a significant (ANOVA, $^{**}P < 0.01$; $^{*}P < 0.5$) difference from the wild type.

miR396s in Arabidopsis roots, revealing that miR396a and miR396b accumulated in different root cell types. miR396a accumulated in the columella and endodermis, whereas miR396b was enriched in the cortex (Breakfield et al. 2012). These data suggest that *MIR396a* and *MIR396b* might undergo differential post-transcriptional regulation, which would have important implications for the functional specification of these genes in root development. Further studies using newly developed technology such as TALENS or CRISPR might provide more *mir396* mutants, which will help us to understand whether miR396b also plays a role during root development.

Ultimately, miRNA-directed regulation depends on the availability of a particular miRNA and distinct miRNA targets within a given cell type. Among known miR396 targets, promoter activities of four targets have been detected in root tissues (**Fig. 3**). *bHLH74*, *GRF4*, *GRF9* and two *MIR396* genes were transcribed in overlapping regions, while *GRF2* was expressed in the root tip, a region where *MIR396a* and *MIR396b* were not transcribed. This implies that there may be different interaction modes between miR396 and its targets. The interaction between miR396 and its targets, which influences the abundance and spatial distribution of *bHLH74* and/or *GRF* gene transcripts, plays a crucial role in root development.

Following phenotype observation of target mutants, *bHLH74* is considered the most important contributor involved in miR396-mediated root growth regulation. Unlike other conserved targets, such as *GRF* genes, which are found in >30 species, from gymnosperms to monocots and eudicots, *bHLH74* homologs with an miR396 target site could be detected only in the sister families *Brassicaceae* and *Cleomaceae* (Debernardi et al. 2012). Recently, Bazin et al. (2013) identified two *bHLH79* transcription factors with miR396 binding sites in *M. truncatula* by searching degradome sequencing results. The miR396/*bHLH79* nodes were present in species of the Fabidae taxon, including Fabaceae (Rosid I), but not in other dicots or in monocots (Bazin et al. 2013). This demonstrates that conserved miRNAs such as miR396 might 'pick up' functional interactions with extra targets while maintaining their canonical regulation modules (Axtell 2013).

Because the conserved targets of miR396 belong to the *GRF* family of transcription factors, previous research has focused on the function of miR396 in controlling cell proliferation in Arabidopsis leaves. Cell proliferation and polarized cell differentiation along the adaxial–abaxial axis in the primordium is

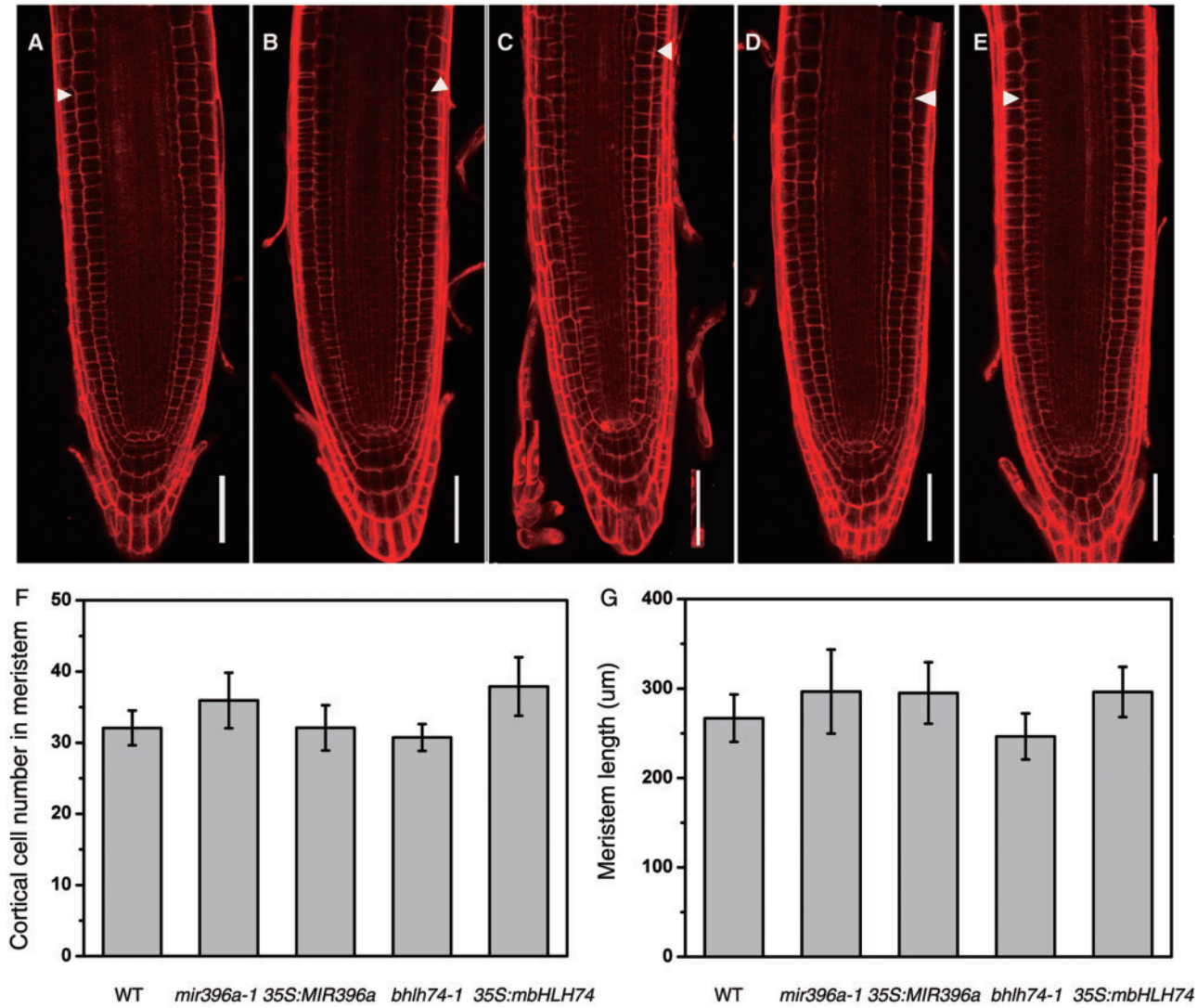


**Fig. 5** miR396 does not affect the root meristem. (A–E) Confocal images of 5-day-old wild-type (A), *mir396a-1* (B), *35S:MIR396a#7* (C), *bhlh74-1* (D) and *35S:mbHLH74#11* (E) roots stained with propidium iodide. Scale bar = 50 μm. The arrowheads indicate the transition zone where cells leave the meristem and enter the elongation zone. (F) Number of meristematic cortex cells in roots of 5-day-old wild-type, *mir396a-1*, *35S:MIR396a #7*, *bhlh74-1* and *35S:mbHLH74 #11* plants. (G) Meristem length in roots of 5-day-old wild-type, *mir396a-1*, *35S:MIR396a #7*, *bhlh74-1* and *35S:mbHLH74#11* plants. The distance between the quiescent center and the first elongating cortical cell corresponds to the meristem size (μm).

critical for leaf morphogenesis (Fleming 2006). The miR396–*GRF* module negatively regulates cell division activity by controlling entry into the mitotic cell cycle and the expression of cell cycle-related genes required for coordination of cell division and differentiation during leaf development in Arabidopsis (Wang et al. 2011). As with leaf development, root growth requires balanced cell proliferation, differentiation and elongation. After seed germination, root cells undergo repeated rounds of division in the root proximal meristem, and then subsequently experience rapid cell expansion in the elongation–differentiation zone (Beemster and Baskin 1998, Ubeda-Tomas et al. 2009, Petricka et al. 2012). Compared with the wild type, *mir396a-1* and *35S:mbHLH74* plants displayed longer roots with an enlarged elongation zone. Conversely, overexpression of *MIR396a* led to inhibition of root growth, with an associated decreased elongation zone length and mature cell size. No remarkable expression changes of cell cycle-related genes were observed in the *mir396a* mutant and overexpression lines (**Supplementary Fig. S7**). Thus, we propose that miR396 regulates root growth via modulation of cell elongation rather than cell proliferation; this is consistent with the expression sites of *AtMIR396* promoters in root tissues. Studies in *Medicago*, however, led to a different conclusion, with overexpression of miR396 in roots resulting in growth inhibition; this correlates with a reduction in cell cycle gene expression and the number of dividing cells in the root apical

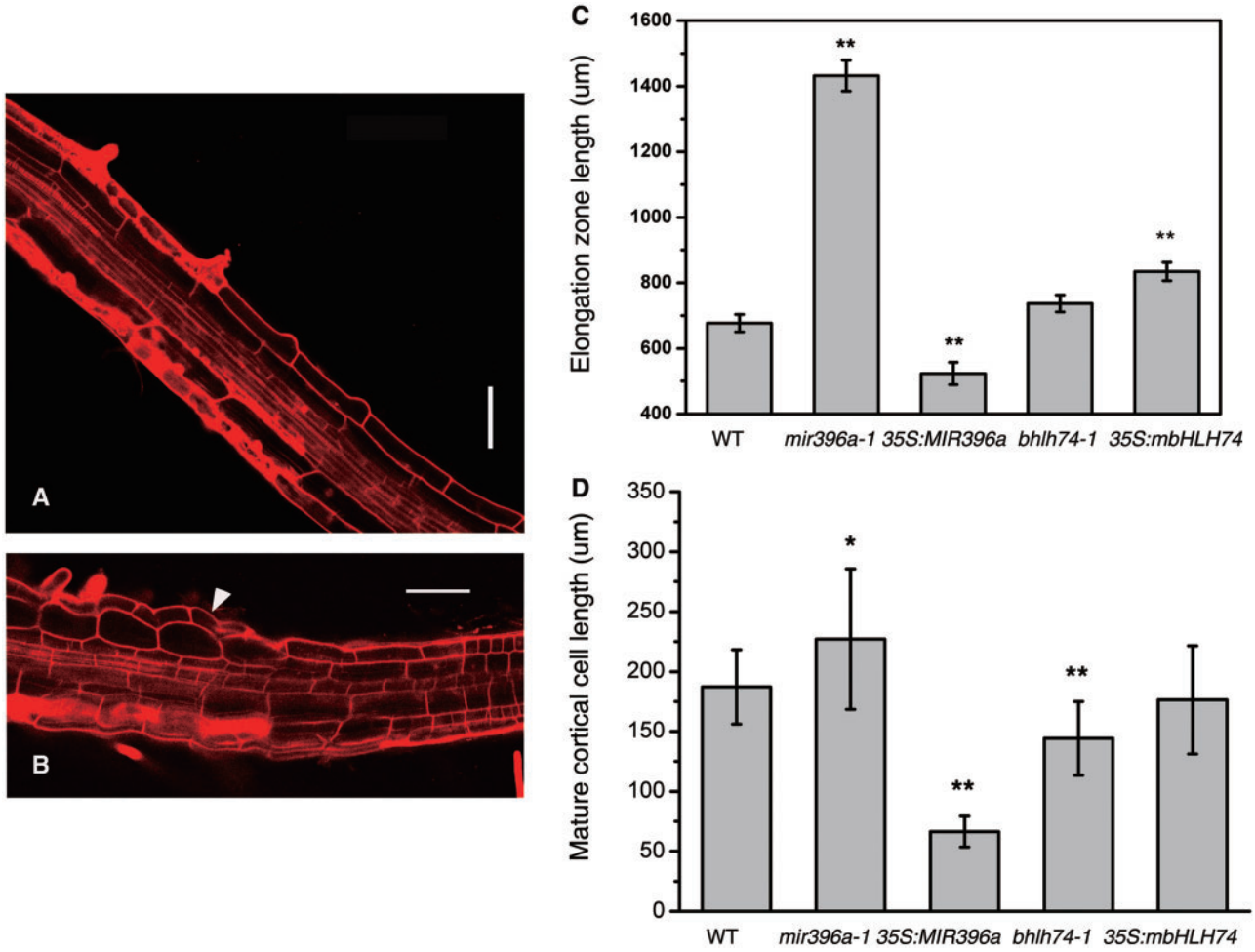


**Fig. 6** miR396 regulates root growth by affecting the elongation zone. Elongation zone of wild-type (A) and *35S:MIR396a #7* (B) roots stained with propidium iodide 5 d after germination. Scale bar = 50 μm. The arrowhead indicates the cell in the elongation zone. (C) Elongation zone length of the wild type, *mir396a-1*, *35S:MIR396a #7*, *bhlh74-1* and *35S:mbHLH74 #11* 5 d after germination. Error bars represent the SD, $n > 20$; asterisks indicate significant differences from wild-type plants, as determined by ANOVA ($^*P < 0.05$; $^{**}P < 0.01$). (D) Mature cortical cell length of the wild type, *mir396a-1*, *35S:MIR396a #7*, *bhlh74-1* and *35S:mbHLH74 #11* 5 d after germination. Error bars represent the SD, $n > 20$; $^*P < 0.05$; $^{**}P < 0.01$.

**Table 1** Primary root length of the *grf* mutants

| Genotype | Primary root length (mm)[a] |
|---|---|
| Wild type (Col-0 background) | 17.4 ± 3.0 |
| Wild type (Ws background) | 14.3 ± 3.1 |
| *grf1grf2grf3* (Ws background) | 15.6 ± 2.2 |
| *grf4* (Col-0 background) | 15.9 ± 2.2 |
| *grf9-1* (Col-0 background) | 17.0 ± 3.2 |

Data are the mean ± SD, for each line; > 30 seedlings were scored.
[a] Average primary root length per plant of 5-day-old seedlings grown on B5 agar plates.

meristem. miR396 seems to act as a regulator of root meristem activity in legumes (Bazin et al. 2013). However, in *Medicago*, impaired root growth was due to repression of three *GRF* targets, but not *MtbHLH79*. Moreover, strong GUS staining was observed for these *GRF* factors in the proximal meristem. These findings indicate that miR396s in different species may interact with different targets to perform their distinct functions.

Although the root phenotype of *grf1grf2grf3*, *grf4* and *grf9-1* mutants seemed normal, genetic experiments and expression pattern analysis suggested that these genes have overlapping functions (Kim et al. 2003, Horiguchi et al. 2005, Kim and Lee 2006, Lee et al. 2009). Therefore, the involvement of GRFs in the regulation of root development cannot be excluded. It is noteworthy that the roots of *bhlh74-1* mutant seedlings were not as short as those from *35S:MIR396a* transgenic plants, and the meristematic and elongation zones in the *bhlh74-1* roots are only slightly different from those of the wild type (**Fig. 4D**). This indicates that there may be other factors besides *bHLH74* targeted by miR396 that participate in root growth regulation.

In addition to root growth, we note that *35S:MIR396a* has more branch roots, and that both *MIR396a* and *bHLH74* promoters were expressed in the emerging lateral roots (**Fig. 3C, E**). These data suggest a potential role for the miR396–*bHLH74* module in lateral root development. In *Medicago*, *MIR396b* displays expression in lateral root and nodule development, and *MIM396* roots have increased dry weight and more branches (Bazin et al. 2013). Further investigation of other miR396–target module roles in root development will enable us to better understand the complexity of this conserved miRNA.

In summary, this study reported that miR396a is involved in regulation of primary root length through interaction with *bHLH74*. *MIR396a* has an additional function as a regulator of root growth in *Arabidopsis* seedlings.

## Materials and Methods

### Plant materials and growth conditions

*Arabidopsis thaliana* ecotype Col-0 was used for all experiments, with the exception of the *grf1grf2grf3* triple mutant, which was analyzed in the Wassilewskija (Ws) background. Plants were grown under long photoperiods (16 h light/8 h dark) at 23°C in growth chambers. For root length analysis, seeds were surface-sterilized and sown on B5 agar plates after synchronization at 4°C for 72 h. Plates were placed vertically in growth chambers. Root elongation was measured using ImageJ software (http://rsb.info.nih.gov/ij/). The T-DNA insertion mutants of *mir396a-1* (SALK_064067) and *grf9-1* (SALK_140746C) were identified independently from the SALK collection (http://signal.salk.edu/). The presence of the T-DNA insertion was determined by PCR using primers LBb1-up or PROK-L located at the left border of the T-DNA- and gene-specific primers. Homozygous plants were identified using gene-specific primers and primers located on the other side of the T-DNA insertion (**Supplementary Table S1**).

### Vector construction and plant transformation

For the *promoter:GUS* constructs, approximately 2 kb sequence upstream from the predicted fold-backs for miR396a and miR396b were amplified by PCR, and used to substitute the *Cauliflower mosaic virus* (CaMV) 35S promoter before the GUS coding sequence in pCAMBIA1301 to obtain *pMIR396a:GUS* and *pMIR396b:GUS*, respectively. For *bHLH74* promoter analysis, the promoter region of *bHLH74*, approximately 2 kb in length, was amplified by PCR from Arabidopsis genomic DNA. The PCR products were transferred into the pENTR/D-TOPO vector (Invitrogen), and subsequently into the destination vector pHGWFS7 containing an *Egfp:uidA* gene fusion by LR clonase reactions according to the manufacturer's instructions. Plasmids for miR396 overexpression were generated by cloning approximately 700 bp genomic fragments of *AtMIR396a* into pCAMBIA13011 harboring the CaMV 35S promoter. To generate an miR396-resistant version of *bHLH74* (*mbHLH74*), the coding sequence of At1g10120 was cloned, and synonymous mutations were introduced into the miR396 binding sequence by overlapping PCR. The resulting product was cloned into pH7FWG2.0. The STTM396 construct used to inactivate miR396 was generated according to Tang et al. (2012). The STTM module, which harbors two short sequences mimicking miR396 target sites linked by a short spacer of 48 nt, was inserted between the CaMV 35S promoter and 35S terminator in pCAMBIA1300. All primers used in this work are listed in **Supplementary Table S1**. The clones used for vector construction were verified by sequencing.

All constructs described were electroporated into *Agrobacterium tumefaciens* GV3101, and used to transform Arabidopsis by the floral dip method (Clough and Bent 1998). Transformants were selected on 12.5 μg ml$^{-1}$ hygromycin (Sigma). Lines containing single insertions were selected based on the segregation ratio of resistant plants; homozygous stocks of $T_3$ seeds were used for this study.

### GUS assays

To visualize the expression of reporters, transgenic plants were subjected to GUS staining by incubating seedlings in a solution of 1 mg ml$^{-1}$ 5-bromo-4-chloro-3-indolyl-β-D-glucuronic acid, 1 mM potassium ferricyanide, 0.1% Triton X-100, 0.1 M sodium phosphate buffer, pH 7.0 and 10 mM EDTA overnight at 37°C, followed by clearing in 70% ethanol.

### Microscopic observation

For root tip observations, seedlings were cleared with chloral hydrate and photographed with Nomarski optics on a Nikon photomicroscope. Confocal images were acquired on an inverted Zeiss LSM 710 Meta microscope after the root was stained with 10 μg ml$^{-1}$ propidium iodide (Sigma-Aldrich). For staining of the columella amyloplasts, roots were immersed in Lugol's solution for 1–2 min. Cortex cell number in the meristem, and the root meristem size were determined as one file of cortex cells extending from the quiescent center to where the cells started to elongate. The elongation zone is between the first elongating cortical cell and the differentiation zone; the latter is indicated by the formation of root hair. Meristem and elongation zone lengths were measured using imageJ software.

### Small RNA analysis

RNA was extracted using TRIzol (Invitrogen) according to the manufacturer's instructions. Total RNA was resolved on 17% polyacrylamide gels under denaturing conditions with 7 M urea. RNA was transferred to HyBond-N+ membranes (Roche) by semi-dry electroblotting (Bio-Rad), and membranes were hybridized to DNA oligonucleotide probes labeled with $^{32}$P using T4 polynucleotide kinase (Fermentas). Alternatively, quantification of mature miR396 levels was carried out through a poly(A)-based real-time PCR approach using a One Step PrimeScript miRNA cDNA Synthesis Kit (TAKARA), and the miR396 level was standardized with that of miR171a (Shi and Chiang 2005).

## Gene expression analysis

Total RNA was treated with DNase I (TAKARA). First-strand cDNA synthesis was carried out using a PrimeScript RT-PCR Kit (TAKARA). PCRs were performed in a Mastercycler ep realplex thermal cycler (Eppendorf) using SYBR Green to monitor double-stranded (ds) DNA synthesis. qRT-PCRs for each gene were performed with at least three biological replicates, and technical duplicates for each biological replicate. Expression levels were normalized against AT4G33380 or *UBQ5* (Czechowski et al. 2005). For semi-quantitative RT-PCR detection of *GRF7*, *GRF8* and *GRF9* in different plant tissues, 3 μg of total RNA was used for reverse transcription. PCR was performed using *ACTIN2* as the control. All primers used for RT-PCR were designed by Primer Premier5 (PREMIER Biosoft) and are listed in **Supplementary Table S1**.

## Supplementary data

**Supplementary data** are available at PCP online.

## Funding

This work was supported by the National Science Foundation of China [grant Nos. 30571197, 31171543, 31171615 and 30972016].

## Acknowledgments

We sincerely thank Dr. Jeong Hoe Kim (Department of Biology, Kyungpook National University, Daegu, Korea) for kindly providing the *grf1grf2grf3* and *grf4* mutants, Dr. Gorou Horiguchi (National Institute for Basic Biology/Okazaki Institute for Integrative Bioscience, Okazaki, Japan) for providing Arabidopsis transgenic lines harboring *promoter:GUS* constructs for *AtGRF1*, *AtGRF2*, *AtGRF3*, *AtGRF4*, *AtGRF7* and *AtGRF9*, and Dr. Javier F. Palatnik (Instituto de Biologia Molecular y Celular de Rosario, Argentina) for supplying *bhlh74-1* (GABI-Kat 720G11).

## Disclosures

The authors have no conflicts of interest to declare.

## References

Axtell, M.J. (2013) Classification and comparison of small RNAs from plants. *Annu. Rev. Plant Biol.* 64: 137–159.

Bazin, J., Khan, G.A., Combier, J.P., Bustos-Sanmamed, P., Debernardi, J.M., Rodriguez, R. et al. (2013) miR396 affects mycorrhization and root meristem activity in the legume Medicago truncatula. *Plant J.* 74: 920–934.

Beemster, G.T. and Baskin, T.I. (1998) Analysis of cell division and elongation underlying the developmental acceleration of root growth in Arabidopsis thaliana. *Plant Physiol.* 116: 1515–1526.

Breakfield, N.W., Corcoran, D.L., Petricka, J.J., Shen, J., Sae-Seaw, J., Rubio-Somoza, I. et al. (2012) High-resolution experimental and computational profiling of tissue-specific known and novel miRNAs in Arabidopsis. *Genome Res.* 22: 163–176.

Carlsbecker, A., Lee, J.Y., Roberts, C.J., Dettmer, J., Lehesranta, S., Zhou, J. et al. (2010) Cell signalling by microRNA165/6 directs gene dose-dependent root cell fate. *Nature* 465: 316–321.

Chen, Z.H., Bao, M.L., Sun, Y.Z., Yang, Y.J., Xu, X.H., Wang, J.H. et al. (2011) Regulation of auxin response by miR393-targeted transport inhibitor response protein 1 is involved in normal development in Arabidopsis. *Plant Mol. Biol.* 77: 619–629.

Clough, S.J. and Bent, A.F. (1998) Floral dip: a simplified method for Agrobacterium-mediated transformation of Arabidopsis thaliana. *Plant J.* 16: 735–743.

Czechowski, T., Stitt, M., Altmann, T., Udvardi, M.K. and Scheible, W.R. (2005) Genome-wide identification and testing of superior reference genes for transcript normalization in Arabidopsis. *Plant Physiol.* 139: 5–17.

Debernardi, J.M., Rodriguez, R.E., Mecchia, M.A. and Palatnik, J.F. (2012) Functional specialization of the plant miR396 regulatory network through distinct microRNA–target interactions. *PLoS Genet.* 8: e1002419.

Fleming, A.J. (2006) The co-ordination of cell division, differentiation and morphogenesis in the shoot apical meristem: a perspective. *J. Exp. Bot.* 57: 25–32.

Guo, H.S., Xie, Q., Fei, J.F. and Chua, N.H. (2005) MicroRNA directs mRNA cleavage of the transcription factor NAC1 to downregulate auxin signals for arabidopsis lateral root development. *Plant Cell* 17: 1376–1386.

Gutierrez, L., Bussell, J.D., Pacurar, D.I., Schwambach, J., Pacurar, M. and Bellini, C. (2009) Phenotypic plasticity of adventitious rooting in Arabidopsis is controlled by complex regulation of AUXIN RESPONSE FACTOR transcripts and microRNA abundance. *Plant Cell* 21: 3119–3132.

Hewezi, T., Maier, T.R., Nettleton, D. and Baum, T.J. (2012) The Arabidopsis microRNA396–GRF1/GRF3 regulatory module acts as a developmental regulator in the reprogramming of root cells during cyst nematode infection. *Plant Physiol.* 159: 321–335.

Horiguchi, G., Kim, G.T. and Tsukaya, H. (2005) The transcription factor AtGRF5 and the transcription coactivator AN3 regulate cell proliferation in leaf primordia of Arabidopsis thaliana. *Plant J.* 43: 68–78.

Jeong, D.H., Thatcher, S.R., Brown, R.S., Zhai, J., Park, S., Rymarquis, L.A. et al. (2013) Comprehensive investigation of microRNAs enhanced by analysis of sequence variants, expression patterns, AGONAUTE loading, and target cleavage. *Plant Physiol.* 162: 1225–1245.

Jones-Rhoades, M.W. and Bartel, D.P. (2004) Computational identification of plant microRNAs and their targets, including a stress-induced miRNA. *Mol. Cell* 14: 787–799.

Jones-Rhoades, M.W., Bartel, D.P. and Bartel, B. (2006) MicroRNAs and their regulatory roles in plants. *Annu. Rev. Plant Biol.* 57: 19–53.

Kim, J.H., Choi, D. and Kende, H. (2003) The AtGRF family of putative transcription factors is involved in leaf and cotyledon growth in Arabidopsis. *Plant J.* 36: 94–104.

Kim, J.H. and Lee, B.H. (2006) GROWTH-REGULATING FACTOR4 of Arabidopsis thaliana is required for development of leaves, cotyledons, and shoot apical meristem. *J. Plant Biol.* 49: 463–468.

Lee, B.H., Ko, J.H., Lee, S., Lee, Y., Pak, J.H. and Kim, J.H. (2009) The Arabidopsis GRF-INTERACTING FACTOR gene family performs an overlapping function in determining organ size as well as multiple developmental properties. *Plant Physiol.* 151: 655–668.

Liu, D., Song, Y., Chen, Z. and Yu, D. (2009) Ectopic expression of miR396 suppresses GRF target gene expression and alters leaf growth in Arabidopsis. *Physiol. Plant.* 136: 223–236.

Lukowitz, W., Mayer, U. and Jurgens, G. (1996) Cytokinesis in the Arabidopsis embryo involves the syntaxin-related KNOLLE gene product. *Cell* 84: 61–71.

Marin, E., Jouannet, V., Herz, A., Lokerse, A.S., Weijers, D., Vaucheret, H. et al. (2010) miR390, Arabidopsis TAS3 tasiRNAs, and their AUXIN RESPONSE FACTOR targets define an autoregulatory network quantitatively regulating lateral root growth. *Plant Cell* 22: 1104–1117.

Meng, Y., Ma, X., Chen, D., Wu, P. and Chen, M. (2010) MicroRNA-mediated signaling involved in plant root development. *Biochem. Biophys. Res. Commun.* 393: 345–349.

Menges, M., de Jager, S.M., Gruissem, W. and Murray, J.A. (2005) Global analysis of the core cell cycle regulators of Arabidopsis identifies novel genes, reveals multiple and highly specific profiles of expression and provides a coherent model for plant cell cycle control. *Plant J.* 41: 546–566.

Petricka, J.J., Winter, C.M. and Benfey, P.N. (2012) Control of Arabidopsis root development. *Annu. Rev. Plant Biol.* 63: 563–590.

Rodriguez, R.E., Mecchia, M.A., Debernardi, J.M., Schommer, C., Weigel, D. and Palatnik, J.F. (2010) Control of cell proliferation in Arabidopsis thaliana by microRNA miR396. *Development* 137: 103–112.

Rubio-Somoza, I., Cuperus, J.T., Weigel, D. and Carrington, J.C. (2009) Regulation and functional specialization of small RNA-target nodes during plant development. *Curr. Opin. Plant Biol.* 12: 622–627.

Shi, R. and Chiang, V.L. (2005) Facile means for quantifying microRNA expression by real-time PCR. *Biotechniques* 39: 519–525.

Tang, G., Yan, J., Gu, Y., Qiao, M., Fan, R., Mao, Y. et al. (2012) Construction of short tandem target mimic (STTM) to block the functions of plant and animal microRNAs. *Methods* 58: 118–125.

Ubeda-Tomas, S., Federici, F., Casimiro, I., Beemster, G.T., Bhalerao, R., Swarup, R. et al. (2009) Gibberellin signaling in the endodermis controls Arabidopsis root meristem size. *Curr. Biol.* 19: 1194–1199.

Vidal, E.A., Araus, V., Lu, C., Parry, G., Green, P.J., Coruzzi, G.M. et al. (2010) Nitrate-responsive miR393/AFB3 regulatory module controls root system architecture in Arabidopsis thaliana. *Proc. Natl Acad. Sci. USA* 107: 4477–4482.

Voinnet, O. (2009) Origin, biogenesis, and activity of plant microRNAs. *Cell* 136: 669–687.

Wang, J.W., Wang, L.J., Mao, Y.B., Cai, W.J., Xue, H.W. and Chen, X.Y. (2005) Control of root cap formation by MicroRNA-targeted auxin response factors in Arabidopsis. *Plant Cell* 17: 2204–2216.

Wang, L., Gu, X., Xu, D., Wang, W., Wang, H., Zeng, M. et al. (2011) miR396-targeted AtGRF transcription factors are required for coordination of cell division and differentiation during leaf development in Arabidopsis. *J. Exp. Bot.* 62: 761–773.

Yan, J., Gu, Y., Jia, X., Kang, W., Pan, S., Tang, X. et al. (2012) Effective small RNA destruction by the expression of a short tandem target mimic in Arabidopsis. *Plant Cell* 24: 415–427.

Yoon, E.K., Yang, J.H., Lim, J., Kim, S.H., Kim, S.K. and Lee, W.S. (2010) Auxin regulation of the microRNA390-dependent transacting small interfering RNA pathway in Arabidopsis lateral root development. *Nucleic Acids Res.* 38: 1382–1391.